

Binuclear Nickel and Copper Complexes with Bridging 2,5-Diamino-1,4-benzoquinonediimines: Synthesis, Structures, and Catalytic Olefin Polymerization

Yuan-Biao Huang, Guang-Rong Tang, Gui-Ying Jin, and Guo-Xin Jin*

Shanghai Key Laboratory of Molecular Catalysis and Innovative Materials, Department of Chemistry, Fudan University, Shanghai, 200 433, People's Republic of China

Received September 10, 2007

A series of binuclear, divalent nickel and copper acetylacetonato complexes of the type $[M(\text{acac})\{\mu\text{-C}_6\text{H}_2(\text{=NAr})_4\}M(\text{acac})]$ ($M = \text{Ni}, \text{Cu}$) have been synthesized by reaction of the corresponding $M(\text{acac})_2$ precursor with various bulky steric hindrance π -acceptor N-substituted 2,5-diamino-1,4-benzoquinonediimines $\text{C}_6\text{H}_2(\text{NHR})_2(\text{=NAr})_2$ (**1a**, $\text{Ar} = 4\text{-C}_6\text{H}_4\text{Me}$; **1b**, $\text{Ar} = 2\text{-C}_6\text{H}_4\text{Me}$; **1c**, $\text{Ar} = 2,6\text{-C}_6\text{H}_3\text{Me}_2$), which are metalated and become bridging ligands. The ligands and complexes were determined by IR and UV–visible spectra and element analysis. Cyclic voltammetric behavior of complexes **2c** and **3c** has been tested. The molecular structures of the ligand **1c** and the complexes $[\text{Ni}(\text{acac})\{\mu\text{-C}_6\text{H}_2(\text{=N}(4\text{-methyl-Ph}))_4\}\text{Ni}(\text{acac})]$ (**2a**), $[\text{Ni}(\text{acac})\{\mu\text{-C}_6\text{H}_2(\text{=N}(2,6\text{-dimethyl-Ph}))_4\}\text{Ni}(\text{acac})]$ (**2c**), and $[\text{Cu}(\text{acac})\{\mu\text{-C}_6\text{H}_2(\text{=N}(2,6\text{-dimethyl-Ph}))_4\}\text{Cu}(\text{acac})]$ (**3c**) have been determined by X-ray diffraction. The coordination geometry around the metal ions of the Ni and Cu complexes is square-planar, and a complete electronic delocalization of the quinonoid π -system occurs between the metal centers over the two $\text{N}=\text{C}-\text{C}=\text{C}=\text{N}$ halves of the ligand. In the presence of MAO as cocatalyst, all the Ni complexes exhibited high activities both for addition polymerization of norbornene and for methyl methacrylate (MMA) polymerization, which produce syndiotactic-rich poly(methyl methacrylate) (PMMA) with broad molecular weight distribution; however, the Cu complexes show moderate activities for norbornene polymerization and are inactive for MMA polymerization.

Introduction

Olefin polymerization of late transition metal catalysts has attracted considerable attention in academic and industrial fields over the past decade.¹ This was triggered by the discovery of highly active α -diimine Ni(II) and Pd(II) precatalysts for ethylene polymerization and oligomerization² and Fe(II) and Co(II) bis(imino)pyridyl-type complexes^{1,3} and single-compo-

nent neutral Ni catalysts.⁴ Other interesting N–N chelating ligands, in particular, β -diketimine⁵ and amino-imine ligands,⁶ have been successfully applied to ethylene oligomerization and polymerization and addition polymerization of norbornene.

Recently, binuclear late transition metal complexes, connected via the extended conjugated π -system of the ligands, have been considered attractive candidates for the occurrence of cooperative effects, which has attracted interest in both academic and industrial sectors.^{7,8} Cooperative effects in catalysis are of great current interest and were recently emphasized by the preparation of highly active binuclear Ni(II) single-component catalysts for

* Corresponding author. E-mail: gxjin@fudan.edu.cn. Fax: +86-21-65641740. Tel: +86-21-65643776.

(1) (a) Britovsek, G. J. P.; Gibson, V. C.; Wass, D. F. *Angew. Chem., Int. Ed.* **1999**, *38*, 428. (b) Ittel, S. D.; Johnson, L. K.; Brookhart, M. *Chem. Rev.* **2000**, *100*, 1169. (c) Gibson, V. C.; Spitzmesser, S. K. *Chem. Rev.* **2003**, *103*, 283. (d) Boffa, L. S.; Novak, B. M. *Chem. Rev.* **2000**, *100*, 1479. (e) Speiser, F.; Braunstein, P.; Saussine, L. *Acc. Chem. Res.* **2005**, *38*, 784. (f) Zhang, J.; Wang, X.; Jin, G.-X. *Coord. Chem. Rev.* **2006**, *250*, 95–109.

(2) (a) Johnson, L. K.; Killian, C. M.; Brookhart, M. *J. Am. Chem. Soc.* **1995**, *117*, 6414–6415. (b) Killian, C. M.; Tempel, D. J.; Johnson, L. K.; Brookhart, M. *J. Am. Chem. Soc.* **1996**, *118*, 11664–11665. (c) Feldman, J.; McLain, S. J.; Parthasarathy, A.; Marshall, W. J.; Calabrese, J. C.; Arthur, S. D. *Organometallics* **1997**, *16*, 1514–1516. (d) Killian, C. M.; Johnson, L. K.; Brookhart, M. *Organometallics* **1997**, *16*, 2005–2007. (e) Mecking, S.; Johnson, L. K.; Wang, L.; Brookhart, M. *J. Am. Chem. Soc.* **1998**, *120*, 888–899. (f) Meinhard, D.; Wegner, M.; Kipiani, G.; Hearley, A.; Reuter, P.; Fischer, S.; Marti, O.; Rieger, B. *J. Am. Chem. Soc.* **2007**, *129*, 9182.

(3) (a) Small, B. L.; Brookhart, M. *J. Am. Chem. Soc.* **1998**, *120*, 7143–7144. (b) Small, B. L.; Brookhart, M.; Bennett, A. M. A. *J. Am. Chem. Soc.* **1998**, *120*, 4049–4050. (c) Britovsek, G. J. P.; Bruce, M.; Gibson, V. C. *J. Am. Chem. Soc.* **1999**, *121*, 8728–8740. (d) Liu, C.-K.; Jin, G.-X. *Acta Chim. Sin.* **2002**, *60*, 157–161. (e) Liu, C.-K.; Jin, G.-X. *New J. Chem.* **2002**, *26*, 1485–1489. (f) Kooistra, T. M.; Hekking, K. F. W.; Knijnenburg, Q.; Bruin, B. D.; Budzelaar, P. H. M.; Gelder, R. d.; Smits, J. M. M.; Gal, A. W. *Eur. J. Inorg. Chem.* **2003**, 648–655. (g) Chen, J.-X.; Huang, Y.-B.; Li, Z.-S.; Zhang, Z.-C.; Wei, C.-X.; Lan, T.-Y.; Zhang, W.-J. *J. Mol. Catal. A: Chem.* **2006**, *259*, 133–141.

(4) (a) Wang, C.; Friedrich, S.; Younkin, T. R.; Li, R. T.; Grubbs, R. H.; Bansleben, D. A.; Day, M. W. *Organometallics*, **1998**, *17*, 3149. (b) Younkin, T. R.; Connor, E. F.; Henderson, J. I.; Friedrich, S. K.; Grubbs, R. H.; Bansleben, D. A. *Science* **2000**, *287*, 460. (c) Hicks, F. A.; Brookhart, M. *Organometallics* **2001**, *20*, 3217. (d) Hicks, F. A.; Jenkins, J. C.; Brookhart, M. *Organometallics* **2003**, *22*, 3533. (e) Jenkins, J. C.; Brookhart, M. *Organometallics* **2003**, *22*, 250. (f) Zhang, D.; Jin, G.-X.; Hu, N.-H. *Chem. Commun.* **2002**, 574. (g) Zhang, D.; Jin, G.-X.; Hu, N.-H. *Eur. J. Inorg. Chem.*, **2003**, 1570. (h) Zhang, D.; Jin, G.-X. *Organometallics* **2003**, *22*, 2851. (i) Zhang, D.; Jin, G.-X. *J. Polym. Sci., Part A: Polym. Chem.* **2004**, *42*, 1018. (j) Zhang, D.; Jin, G.-X.; Weng, L.-H.; Wang, F.-S. *Organometallics* **2004**, *23*, 3270. (k) Zhang, D.; Jin, G.-X. *Appl. Catal., A* **2004**, *262*, 13. (l) Wang, H.-Y.; Jin, G.-X. *Eur. J. Inorg. Chem.* **2005**, 1665. (m) Benedikt, G. M.; Elce, E.; Goodall, B. L.; McIntosh, L. H.; Rhodes, L. F.; Selvy, K. T.; Andes, C.; Oyler, K.; Sen, A. *Macromolecules* **2002**, *35*, 8978–8988.

(5) Bourget-Merle, L.; Lappert, M.; Severn, J. R. *Chem. Rev.* **2002**, *102*, 3031–3065.

(6) (a) Wang, H.-Y.; Meng, X.; Jin, G.-X. *Dalton Trans.* **2006**, 2579–2585. (b) Gao, H.; Guo, W.; Bao, F.; Gui, G.; Zhang, J.; Zhu, F.; Wu, Q. *Organometallics* **2004**, *23*, 6273–6280.

(7) Small, B. L. *Organometallics* **2003**, *22*, 3178–3183.

(8) Chauvin, Y.; Olivier, H. In *Applied Homogeneous Catalysis with Organometallic Compounds*; Cornils, B., Herrmann, W. A., Eds.; VCH: Weinheim, Germany, 1996; Vol. 1, pp 258–268.

ethylene polymerization containing 2,5-disubstituted amino-*p*-benzoquinone ligands,^{4b} 3,3'-bisalicylaldimine ligands,⁹ homobinuclear oxalamidinato Ni and Pd complexes,¹⁰ and small steric hindrance 2,5-diamino-1,4-benzoquinonedimine Ni and Pd complexes.¹¹

The NB (norbornene) addition polymer displays a characteristic rigid random coil conformation, which shows restricted rotation about the main chain and exhibits high thermal stability ($T_g > 350$ °C). In addition, it has excellent dielectric properties, optical transparency, and unusual transport properties.^{1b,c} Therefore, it has been attracting many chemists to study NB addition polymerization. Up to now, catalytic systems based on titanium,¹² zirconium,¹³ hafnium,¹⁴ vanadium,¹⁵ cobalt,^{3g,16} chromium,^{3g,17,18} nickel,^{4l,5,6,18–21} and palladium^{21j,22–24} have been mainly reported for the addition polymerization of NB. Recently, rare-earth metals were also used in this reaction, although with low activity.²⁵

Late transition metal complexes, due to their less oxophilic nature relative to early transition metal complexes, are generally considered to be more tolerant toward polar functional monomers, which makes them likely targets for the development of catalysts for the polymerization of polar monomers including methyl methacrylate (MMA).¹ Gibson reported Ni(acac)₂-catalyzed generation of Schiff base aluminum enolate initiators for controlled MMA polymerization.²⁶ A series of nickel(II)

complexes bearing N,O-chelate ligand activation with MAO for MMA polymerization yield PMMA with rich syndiotacticity microstructure.²⁷ Yasuda reported that a series of organo-nickel complexes activated with MMAO exhibited high catalytic activity for the polymerization of MMA.²⁸ The Ni(acac)₂/MAO catalyst system was found to be an effective catalyst for the polymerization of MMA.^{29a,c} Kim et al.^{29d} reported that late transition metal complexes such as (α -diimine)nickel, (pyridyl bisimine)iron(II), and (pyridyl bisimine)cobalt(II) complexes activated with MAO can polymerize MMA and obtained syndiotactic-rich PMMA.

To date, reports on olefin polymerization catalysts based on copper are scarce.^{1c} The α -diimine Cu(II) complex produces very high molecular weight PE with moderate activity.³⁰ The benzamidinate complex and the benzimidazole complex both show low activity for ethylene polymerization.³¹ The benzimidazole complexes are also able to produce acrylate-rich ethylene-acrylate copolymers with very low activities.^{32,33} The Carlini group found that bis(salicylaldimine)copper(II) complexes activated with MAO can catalyze norbornene polymerization and obtained high molecular weight addition-type polymers.³⁴ The bis(salicylaldimine)copper(II) complexes activated with MAO can also catalyze the homo- and copolymerizations of ethylene and methyl methacrylate (MMA).³⁵ Copper complexes bearing N,O-chelating β -ketoamine ligands based on condensation products of 1-phenyl-3-methyl-4-benzoyl-5-pyrazolone with a series of amines were shown to catalyze the addition polymerization of norbornene when activated by methylaluminumoxane.³⁶ Our group also reported that the copper complex bearing 2'-(4',6'-di-*tert*-butylhydroxyphenyl)-1,4,5-triphenyl imidazole^{37a} and hydroxyindanimine^{37b} ligands activated with MAO catalyze addition polymerization of norbornene with moderate activity.

Although azophenine (R = Ph) was synthesized as early as 1875,³⁸ the coordination chemistry of the closely related 2,5-

(9) Hu, T.; Tang, L.-M.; Li, X.-F.; Li, Y.-S.; Hu, N.-H. *Organometallics* **2005**, *24*, 2628–2632.

(10) (a) Döhler, T.; Görls, H.; Walther, D. *Chem. Commun.* **2000**, *94*, 5–946. (b) Walther, D.; Döhler, T.; Theysen, N.; Görls, H. *Eur. J. Inorg. Chem.* **2001**, 2049–2060. (c) Rau, S.; Lamm, K.; Görls, H.; Schöffel, J.; Walther, D. *J. Organomet. Chem.* **2004**, *689*, 3582–3592.

(11) Taquet, J. P.; Siri, O.; Braunstein, P. *Inorg. Chem.* **2006**, *45*, 4668. (12) Tritto, I.; Boggioni, L.; Sacchi, M. C.; Locatelli, P. *J. Mol. Catal. A: Chem.* **1998**, *133*, 139.

(13) Kaminsky, W.; Bark, A.; Arndt, M. *Makromol. Chem., Macromol. Symp.* **1991**, *47*, 83.

(14) Brekner, M. J.; Decker, H.; Osan, F. (Hoechst AG) EP Patent 683,797, 1994.

(15) Minchak, R. J.; Ware, J. T. (B. F. Goodrich) EP Patent 291,970, 1988.

(16) (a) Goodall, B. L.; McIntosh, L. H., III; Rhodes, L. F. *Makromol. Chem., Macromol. Symp.* **1995**, *89*, 421. (b) Yasuda, H.; Nakayama, Y.; Sato, Y. *J. Organomet. Chem.* **2004**, *689*, 744–750. (c) Frédéric, P.; Pierre, J. L.; Marcel, W.; Jacky, K. *Macromol. Rapid Commun.* **2003**, *24*, 768–771.

(17) Peuckert, U.; Heitz, W. *Macromol. Rapid Commun.* **1998**, *19*, 159.

(18) Lassahn, P.-G.; Lozan, V.; Timco, G. A.; Christian, P.; Janiak, C.; Winpenny, E. P. *J. Catal.* **2004**, *222*, 261.

(19) Barnes, D. A.; Benedikt, G. M.; Goodall, B. L.; Huang, S. S.; Kalamirides, H. A.; Lenhard, S.; McIntosh, L. H., III; Selvy, K. T.; Shick, R. A.; Rhodes, L. F. *Macromolecules* **2003**, *36*, 2623.

(20) Lozan, V.; Lassahn, P.-G.; Zhang, C.; Wu, B.; Janiak, C.; Rheinwald, G.; Lang, H. Z. *Naturforsch. B* **2003**, *58*, 1152.

(21) (a) Janiak, C.; Lassahn, P. G. *J. Mol. Catal. A: Chem.* **2001**, *166*, 193–209. (b) Zhu, Y.-Z.; Liu, J.-Y.; Li, Y.-S.; Tong, Y.-J. *J. Organomet. Chem.* **2004**, *689*, 1295. (c) Hou, J.-X.; Sun, W.-H.; Zhang, D.-H.; Chen, L.-Y. *J. Mol. Catal. A: Chem.* **2005**, *231*, 221–233. (d) Chang, F.; Zhang, D.; Xu, G.-Y.; Yang, H.-J.; Li, J.-T.; Song, H.-B.; Sun, W.-H. *J. Organomet. Chem.* **2004**, *689*, 936–946. (e) Suzuki, H.; Matsumura, S.; Satoh, Y.; Sogoh, K.; Yasuda, H. *React. Funct. Polym.* **2004**, *58*, 77–91. (f) Mi, X.; Ma, Z.; Cui, N.; Wang, L.; Ke, Y.; Hu, Y. *J. Appl. Polym. Sci.* **2003**, *88*, 3273–3278. (g) Wang, X.; Liu, S.; Jin, G.-X. *Organometallics* **2004**, *23*, 6002–6007. (h) Wang, X.; Jin, G.-X. *Organometallics* **2004**, *23*, 6319–6322. (i) Wang, W.-H.; Jin, G.-X. *Inorg. Chem. Commun.* **2005**, *8*, 109–112. (j) Janiak, C.; Lassahn, P. G.; Lozan, V. *Macromol. Symp.* **2006**, *236*, 88–99.

(22) Mehler, C.; Risse, W. *Macromolecules* **1992**, *25*, 4226.

(23) Lassahn, P.-G.; Lozan, V.; Janiak, C. *Dalton Trans.* **2003**, 927.

(24) Berchtold, B.; Lozan, V.; Lassahn, P.-G.; Janiak, C. *J. Polym. Sci. A: Polym. Chem.* **2002**, *40*, 3604.

(25) Karl, M.; Seybert, G.; Massa, W.; Harms, K.; Agarwal, S.; Maleika, R.; Stelter, W.; Greiner, A.; Heitz, W.; Neumuller, B.; Dehnicke, K. Z. *Anorg. Allg. Chem.* **1999**, *625*, 1301.

(26) Cameron, P. A.; Gibson, V. C.; Irvine, D. J. *Angew. Chem., Int. Ed.* **2000**, *39*, 2141.

(27) (a) He, X.; Yao, Y.; Luo, X.; Zhang, J.; Liu, Y.; Zhang, L.; Wu, Q. *Organometallics* **2003**, *22*, 4952–4957. (b) Carlini, C.; Martinelli, M.; Galletti, A. M. R.; Sbrana, G. *J. Polym. Sci. A: Polym. Chem.* **2003**, *41*, 2117–2124. (c) Tang, G.-R.; Jin, G.-X. *Dalton Trans.* **2007**, 3840–3846. (d) Carlini, C.; Martinelli, M.; Passaglia, E.; Galletti, A. M. R.; Sbrana, G. *Macromol. Rapid Commun.* **2001**, *22*, 664–668. (e) Carlini, C.; Martinelli, M.; Galletti, A. M. R.; Sbrana, G. *J. Polym. Sci. A: Polym. Chem.* **2003**, *41*, 1716–1724. (f) Carlini, C.; Luise, V. D.; Martinelli, M.; Galletti, A. M. R.; Sbrana, G. *J. Polym. Sci. A: Polym. Chem.* **2006**, *44*, 620–633.

(28) Ihara, E.; Fujimura, T.; Yasuda, H.; Maruo, T.; Kanehisa, N.; Kai, Y. *J. Polym. Sci.: Part A: Polym. Chem.* **2000**, *38*, 4764–4775.

(29) (a) Endo, K.; Inukai, A. *Polym. Int.* **2000**, *49*, 110–114. (b) Endo, K.; Inukai, A.; Otsu, T. *Macromol. Rapid Commun.* **1994**, *15*, 897. (c) Coutinho, F. M. B.; Costa, M. A. S.; Monteiro, L. F.; Maria, L. C. *Polym. Bull.* **1997**, *38*, 303. (d) Kim, I.; Hwang, J.-M.; Lee, J. K.; Ha, C. S.; Woo, S. I. *Macromol. Rapid Commun.* **2003**, *24*, 508.

(30) Gibson, V. C.; Tomov, A.; Wass, D. F.; White, A. J. P.; Williams, D. J. *J. Chem. Soc., Dalton Trans.* **2002**, 2261–2262.

(31) Shibayama, M. (Sekisui Chemical Co., Ltd., Japan). PCT Int. Appl. WO9835996, 1998; *Chem. Abstr.* **1998**, *129*, 03390.

(32) Saunders, B. L.; Joseph, S. A.; Smita, K.; Enock, B.; Robert, S. T.; Schulz, D. N.; Rucker, S. P. *J. Polym. Sci. Part A: Polym. Chem.* **2006**, *44*, 1817–1840.

(33) Stibrany, R. T.; Schulz, D. N.; Kacker, S.; Patil, A. O.; Baugh, L. S.; Rucker, S. P.; Zushma, S.; Berluce, E.; Sissano, J. A. *Macromolecules* **2003**, *36*, 8584–8586.

(34) Carlini, C.; Giaiacopi, S.; Marchetti, F.; Pinzino, C.; Galletti, A. M. R.; Sbrana, G. *Organometallics* **2006**, *25*, 3659–3664.

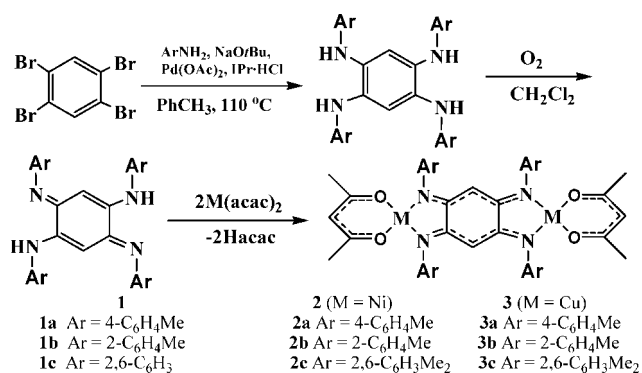
(35) Galletti, A. M. R.; Carlini, C.; Giaiacopi, S.; Marco, M.; Glauco, S. *J. Polym. Sci. Part A: Polym. Chem.* **2007**, *45*, 1134–1142.

(36) Lü, X.-Q.; Bao, F.; Kang, B.-S.; Wu, Q.; Liu, H.-Q.; Zhu, F.-M. *J. Organomet. Chem.* **2006**, *691*, 821–828.

(37) (a) Chen, F.-T.; Tang, G.-R.; Jin, G.-X. *J. Organomet. Chem.* **2007**, *692*, 3435–3442. (b) Tang, G.-R.; Lin, Y.-J.; Jin, G.-X. *J. Organomet. Chem.* **2007**, *692*, 4106.

(38) Kimish, C. *Ber. Dtsch. Chem. Ges.* **1875**, *8*, 1026.

Scheme 1. Synthesis of 1a–c, 2a–c, and 3a–c



diamino-1,4-benzoquinonediimines has remained poorly explored, and only 12 complexes have been reported in the literature.^{11,39} Binuclear Ni and Pd complexes containing 2,5-diamino-1,4-benzoquinone-diimines with various N-substituents (R = Ph, CH_2t -Bu, CH_2Ph) were prepared to explore the coordination properties of the amino- and imino-type donor groups, examine the extent of electronic delocalization of the π -system through the bridge, and evaluate their catalytic oligomerization of ethylene.¹¹

In this paper, we describe the preparation, structures, and properties of norbornene addition polymerization and polymerization of methyl methacrylate of the binuclear nickel and copper acetylacetonato (acac) complexes of the type $[M(acac)\{\mu-C_6H_2(=NAr)_4\}M(acac)]$ (M = Ni, Cu) containing various bulky steric hindrance π -acceptor N-substituents 2,5-diamino-1,4-benzoquinone-diimines (**1a**, Ar = 4- C_6H_4Me ; **1b**, Ar = 2- C_6H_4Me ; **1c**, Ar = 2,6- $C_6H_3Me_2$).

Results and Discussion

Synthesis and Characterization of Binuclear Ni^{II} and Cu^{II} Complexes. The ligands (**1a**, Ar = 4- C_6H_4Me ; **1b**, Ar = 2- C_6H_4Me ; **1c**, Ar = 2,6- $C_6H_3Me_2$) were synthesized according to the method of Buchwald–Hartwig Pd-catalyzed cross-coupling amination of 1,2,4,5-tetrabromobenzene with aromatic amines under basic conditions,⁴⁰ as shown in Scheme 1, and were different from the reported ligands 2,5-diamino-1,4-benzoquinonediimine $C_6H_2(=NR)_2(NHR)_2$ (R = CH_2t -Bu, CH_2Ph , Ph).¹¹ The reaction was performed in toluene with 1,3-bis(2,6-diisopropylphenyl)imidazolylidene·HCl⁴¹ (IPr·HCl): Pd(OAc)₂ (2:1 stoichiometry; 2 mol % Pd catalyst relative to 1,2,4,5-tetrabromobenzene) as the catalyst (Scheme 1). The tetraamine was dissolved in CH_2Cl_2 and stirred under an atmosphere of oxygen at room temperature, giving the ligands 2,5-diamino-1,4-benzoquinonediimine $C_6H_2(NHAr)_2(=NAr)_2$ (**1a**, **1b**, and **1c**). At 25 °C the azophenine derivatives **1a–c** showed single N–H proton resonances, indicative of rapid

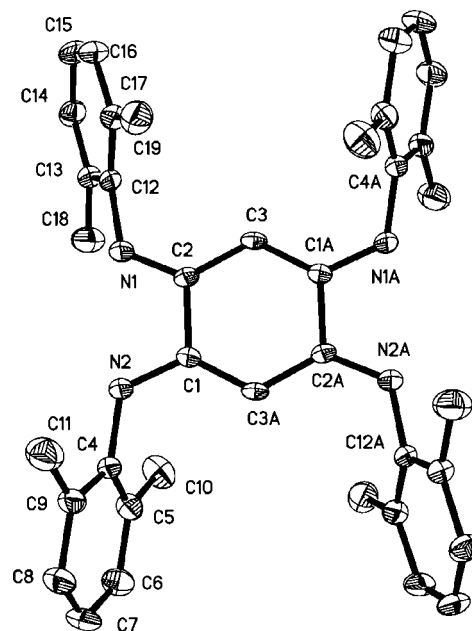


Figure 1. Molecular structure of the ligand **1c** with thermal ellipsoids at the 30% probability level. All H atoms have been omitted for clarity. The symmetry codes are A: $-x+1$, $-y+1$, $-z+1$.

tautomerization on the NMR time scale.^{40c,42} These resonances occur at 8.19, 8.23, and 7.84 for **1a**, **1b**, and **1c** in $CDCl_3$, respectively. The IR shifts were also in the expected region (**3a**: $\nu_{N-H} = 3317\text{ cm}^{-1}$; **3b**: $\nu_{N-H} = 3240\text{ cm}^{-1}$; **3c**: $\nu_{N-H} = 3291\text{ cm}^{-1}$).

The crystal structure of the ligand **1c**, which was grown by the slow evaporation from CH_2Cl_2 solution, was determined by X-ray diffraction (Figure 1). The four N atoms and the central ring are coplanar; the N(1)–C(1) and N(2)–C(2) bond lengths are 1.341(4) and 1.291(4) Å, respectively. The bond length of 1.500(4) Å between C(1) and C(2) is significantly longer than the C(2)–C(3) and C(3)–C(1A) bond lengths of 1.415(5) and 1.355(5) Å. Thus the molecule may be described as composed of two equivalent, delocalized, six-electron π -systems (the N(1)–C(1)–C(3A)–C(2A)–N(2A) unit and the N(2)–C(2)–C(3)–C(1A)–N(1A) unit), which are not conjugated but are joined by C–C bonds.^{40,43} The angles of the plane formed by the four N atoms and the plane of the phenyl rings (C4 to C9, C12 to C17) are 71.7° and 72.8°, respectively.

The purple binuclear Ni^{II} complexes **2** were obtained in good yields from the reaction between the corresponding nickel acetylacetonate precursor and the ligands **1a–c**, respectively, in CH_2Cl_2 (Scheme 1). The ¹H NMR spectra of **2a**, **2b**, and **2c** revealed the presence of four magnetically equivalent methyl groups of the acetylacetonate part and no NH resonance. This is consistent with a bis-chelating, tetradentate behavior for the dianionic ligand derived from **1a** and **1b** and with a fully delocalized π -system. The N–H stretch in the IR spectra of complexes **2a–c** was absent.

Similarly, the Cu^{II} complexes **3** were obtained in good yields from the reaction between the corresponding copper acetylacetonate precursor and the ligands **1a–c**, respectively, in CH_2Cl_2

(39) (a) Rall, J.; Stange, A. F.; Hübler, K.; Kaim, W. *Angew. Chem., Int. Ed.* **1998**, *37*, 2681. (b) Frantz, S.; Rall, J.; Hartenbach, I.; Schleid, T.; Zalis, S.; Kaim, W. *Chem.–Eur. J.* **2004**, *10*, 149. (c) Braunstein, P.; Demessence, A.; Siri, O.; Taquet, J.-p.; *C. R. Chim.* **2004**, *7*, 909. (d) Siri, O.; Braunstein, P. *Chem. Commun.* **2000**, 2223. (e) Siri, O.; Taquet, J.-p.; Collin, J.-P.; Rohmer, M.-M.; Bénard, M.; Braunstein, P. *Chem.–Eur. J.* **2005**, *11*, 7247. (f) Siri, O.; Braunstein, P.; Taquet, J.-P.; Collin, J. P.; Welter, R. *Dalton Trans.* **2007**, 1481–1483.

(40) (a) Khramov, D. M.; Boydston, A. J.; Bielawski, C. W.; *Org. Lett.* **2006**, *8*, 1831. (b) Boydston, A. J.; Khramov, D. M.; Bielawski, C. W.; *Tetrahedron Lett.* **2006**, *47*, 5123. (c) Wenderski, T.; Light, K. M.; Ogrin, D.; Bott, S. G.; Harlan, C. J. *Tetrahedron Lett.* **2004**, *45*, 6851–6853.

(41) Hillier, A. C.; Grasa, G. A.; Viciu, M. S.; Lee, H. M.; Yang, C.; Nolan, S. P. *J. Organomet. Chem.* **2002**, *653*, 69.

(42) Rumpel, H.; Limbach, H. H. *J. Am. Chem. Soc.* **1989**, *111*, 5429–5441.

(43) (a) Siri, O.; Braunstein, P.; Rohmer, M.-M.; Bénard, M.; Welter, R. *J. Am. Chem. Soc.* **2003**, *125*, 13793–13803. (b) Braunstein, P.; Siri, O.; Taquet, J.; Rohmer, M.-M.; Bénard, M.; Welter, R. *J. Am. Chem. Soc.* **2003**, *125*, 12246–12256.

Table 1. Crystallographic Data for 1c, 2a, 2c, and 3c

	1c	2a	2c	3c
empirical formula	C ₃₈ H ₄₀ N ₄	C ₄₄ H ₄₈ N ₄ O ₆ Ni ₂	C ₄₈ H ₅₂ N ₄ O ₄ Ni ₂	C ₄₈ H ₅₂ N ₄ O ₄ Cu ₂
fw	552.74	846.28	866.36	876.02
cryst syst	triclinic	monoclinic	triclinic	triclinic
space group	<i>P</i> $\bar{1}$	<i>C</i> 2/ <i>m</i>	<i>P</i> $\bar{1}$	<i>P</i> $\bar{1}$
<i>a</i> (Å)	8.483(5)	23.63(3)	7.651(2)	7.688(3)
<i>b</i> (Å)	9.652(5)	7.308(9)	11.783(3)	11.813(5)
<i>c</i> (Å)	10.570(7)	16.31(2)	13.848(4)	13.804(5)
α (deg)	81.832(12)	90	114.862(4)	114.828(6)
β (deg)	66.426(7)	128.656(17)	99.241(5)	99.704(6)
γ (deg)	74.004(9)	90	90.263(5)	90.174(6)
<i>V</i> (Å ³)	762.0(8)	2200(5)	1114.4(6)	1117.8(8)
<i>Z</i>	1	2	1	1
<i>D</i> _{calc} (Mg m ⁻³)	1.204	1.278	1.291	1.301
cryst size (mm)	0.12 × 0.10 × 0.08	0.10 × 0.08 × 0.05	0.15 × 0.10 × 0.10	0.15 × 0.12 × 0.02
μ (mm ⁻¹)	0.071	0.905	0.891	0.998
<i>F</i> (000)	296	888	456	458
θ_{\max} , θ_{\min} (deg)	27.19, 2.10	25.01, 1.6	25.01, 1.65	27.19, 1.65
index range <i>h</i>	−7→10	−28→30	−8→9	−9→9
<i>k</i>	−12→11	−9→8	−14→11	−11→15
<i>l</i>	−13→13	−21→18	−16→16	−17→13
<i>R</i> _{int}	0.0340	0.1778	0.0385	0.0262
no. of indep reflns	3304	2077	3870	4733
no. of obsd reflns	3906	3794	4720	5588
no. of variables	198	167	268	268
final <i>R</i> indices [<i>I</i> > 2 σ (<i>I</i>): <i>R</i> ₁ , <i>wR</i> ₂	0.0877, 0.2175	0.1341, 0.3082	0.0663, 0.1446	0.0533, 0.1200
final <i>R</i> indices [all data]: <i>R</i> ₁ , <i>wR</i> ₂	0.1410, 0.2351	0.2626, 0.3778	0.1081, 0.1627	0.0967, 0.1437
GOF	1.207	0.975	0.992	0.986
largest diff peak (hole) (e Å ⁻³) ^a	0.318 (−0.258)	1.184 (−1.009)	0.703 (−0.357)	0.361 (−0.273)

^a Largest peak (hole) in difference Fourier map, $R_1 = \sum(|F_o| - |F_c|)/\sum|F_o|$, $wR_2 = \sum(|F_o|^2 - |F_c|^2)/\sum(F_o^2)^{1/2}$.

Table 2. Selected Bond Lengths (Å) for 1c, 2a, 2c, and 3c

	1c	2a	2c	3c
C1–C2	1.500(4)	1.417(18)	1.501(6)	1.506(5)
C2–C3	1.415(5)	1.399(2)	1.380(6)	1.381(5)
C1–C3A	1.355(5)	1.3495(16)	1.383(6)	1.405(4)
N1–C1	1.341(4)	1.3174(19)	1.328(6)	1.313(4)
N2–C2	1.291(4)	1.3389(15)	1.323(5)	1.300(4)
M–N1		1.900(3)	1.863(4)	1.932(3)
M–N2		1.890(3)	1.881(4)	1.940(3)
M–O1		1.858(3)	1.832(3)	1.910(3)
M–O2		1.879(3)	1.843(3)	1.899(3)

Table 3. Selected Bond Angles (deg) for 1c, 2a, 2c, and 3c

	1c	2a	2c	3c
C1–N1–C4	123.4(3)	120.65(10)	120.3(4)	119.1(3)
C2–N2–C12(C11)	122.9(3)	122.94(12)	119.8(4)	120.4(3)
N1–C1–C2	113.4(3)	113.36(10)	111.7(4)	113.9(3)
N2–C2–C1	115.1(3)	114.17(13)	112.3(4)	112.7(3)
N1–M1–N2		82.05(6)	83.50(16)	81.96(12)
O1–M1–N2		174.27(3)	173.12(15)	176.39(12)
O1–M1–N1		92.22(7)	89.64(15)	94.91(12)
O2–M1–N2		90.08(4)	92.38(15)	90.69(12)
O2–M1–N1		172.13(3)	175.66(16)	172.56(12)
O2–M1–O1		95.65(5)	94.49(15)	92.47(11)

(Scheme 1). ¹H NMR analysis failed due to the paramagnetic character of the Cu(II) complex, which is similar to the bis(salicylaldiminate)copper(II) complexes³⁴ and copper complexes bearing 2'-(4',6'-di-*tert*-butylhydroxyphenyl)-1,4,5-triphenyl imidazole^{37a} and hydroxyindanimine.^{37b} The IR and elemental analyses were measured, and the N–H stretch was absent. The elemental analysis results revealed that the components of all complexes were in accord with the formula Cu(acac){ μ -C₆H₂(=NAr)₄}Cu(acac). The formation of Ni^{II} and Cu^{II} coordination oligomers was not observed in the reactions, indicating the stability and reduced reactivity of the acac ligands in complexes **2** and **3**, as was also observed in the related Ni^{II} and Pd^{II} systems.^{10b,11} All the complexes of **2** and **3** are slightly soluble in CH₂Cl₂, THF, and chlorobenzene and insoluble in diethyl ether and hydrocarbons. However, crystals suitable for X-ray crystallography of the **2a**, **2c**, and **3c** were obtained by slow evaporation from CH₂Cl₂/hexane (10:1) solution. A single crystal of nickel complex **2a** suitable for X-ray structure determination was very difficult to obtain due to its poor solubility; the high *R*₁ [*I* > 2 σ (*I*)] value was difficult to refine well. Crystallographic data and selected bond lengths and angles are given in Tables 1–3.

The molecular structure of **2a** (Figure 2) consists of a binuclear centrosymmetric unit in which the 4N bridging ligand behaves as a bischelate and bridges two (acac)Ni^{II} fragments. The coordination geometry around the nickel center is exact

square-planar. As can be seen from Table 2, by comparison with the bonding parameters, the N1–C1–C3A–C2A–N2A and N2–C2–C3–C1A–N1A moieties are consistent with an extensive electronic delocalization, but there is no conjugation between these two 6 π -systems, since the C1–C2 distance (1.417(18) Å) corresponds to a typical single bond.^{11,39d,e} The Ni1...Ni1A distance of 7.6968(78) Å is slightly longer than that found in the binuclear nickel complex [(acac)Ni{ μ -C₆H₂(=NCH₂*t*-Bu)₄}Ni(acac)] (7.62(2) Å).^{39e} The bond lengths of Ni–N (1.900(3), 1.890(3) Å) are longer than the δ -donor alkyl group substituted complex [(acac)Ni{ μ -C₆H₂(=NCH₂*t*-Bu)₄}Ni(acac)] (1.876(2), 1.877(2) Å)^{39e} and [(acac)Ni{ μ -C₆H₂(=NCH₂Ph)₄}Ni(acac)] (1.874(3), 1.875(3) Å).¹¹ The phenyl rings of the N-substituents (C4 to C5A, C9 to C11A) are almost oriented essentially orthogonal to the plane formed by the four N atoms (90° and 95.2°), and the dihedral angle between the two phenyl rings (C4 to C5A, C9 to C11A) is 36.3°.

The solid structure of **2c** (Figure 3) is very similar to that of complex **2a**. As expected, the coordination geometry around the Ni centers can be seen as square-planar (the dihedral angle between N1–Ni1–N2 and O1–Ni1–O2 is 1.4°, which is bigger than in **2a**; the Ni1 deviates from the [O1, O2, N1, N2] plane by 0.0073 Å). The Ni(1)...Ni(1A) distance is 7.6533(18) Å, which is slightly shorter than in complex **2a** (7.6968(78) Å) and nickel complex [(acac)Ni{ μ -C₆H₂(=NCH₂*t*-Bu)₄}Ni(acac)]

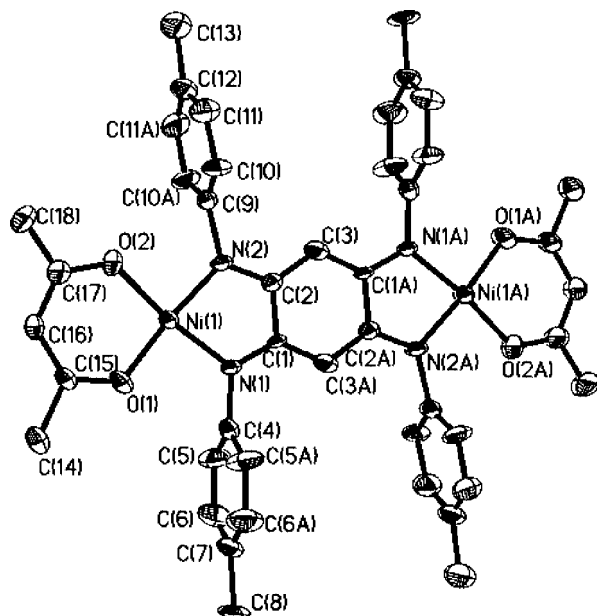


Figure 2. Molecular structure of the Ni complex **2a** with thermal ellipsoids at the 30% probability level. All H atoms and H₂O have been omitted for clarity. The symmetry codes are A: $-x+1, -y+2, -z+2$.

(7.62(2) Å).^{39e} Both of the bond lengths Ni1–N1 and Ni1–N2 (1.863(4), 1.881(4) Å) are shorter than that of the Ni complex **2a** (1.900(3), 1.890(3) Å) and Pd complex [(acac)Pd{ μ -C₆H₂(=NCH₂*t*-Bu)₄}Pd(acac)] (1.984(2), 1.987(3) Å),¹¹ and Ni1–N1 (1.863(4) Å) is shorter than the δ -donor alkyl group substituted complexes [(acac)Ni{ μ -C₆H₂(=NCH₂*t*-Bu)₄}Ni(acac)] (1.876(2) Å) and [(acac)Ni{ μ -C₆H₂(=NCH₂Ph)₄}Ni(acac)] (1.874(3) Å), but the bond length Ni1–N2 is longer than in the complexes [(acac)Ni{ μ -C₆H₂(=NCH₂*t*-Bu)₄}Ni(acac)] (1.877(2) Å)^{39e} and [(acac)Ni{ μ -C₆H₂(=NCH₂Ph)₄}Ni(acac)] (1.875(3) Å).¹¹ The phenyl rings of the N-substituents (C4 to C9, C12 to C17) are almost oriented essentially orthogonal to the plane formed by the four N atoms (93.1° and 80.9°), which are larger than in the corresponding ligand **1c**. The dihedral angle of 26.1° between the two phenyl rings (C4 to C9, C11 to C16) is larger than in complex **2a** (11.9°).

The solid structure of dark green Cu complex **3c** is also similar to the Ni complexes **2a** and **2c**. The coordination geometry around the copper center is square-planar (Figure 4). The Cu1 atom deviates by 0.087 and 0.0439 Å from the plane of the four N atoms and the plane of the acac. The Cu1...Cu1A distance is 7.6880(31) Å, which is longer than in Ni complex **2c** (7.6533(18) Å). As can be seen from Table 2, both the bond lengths Cu1–N1 (1.932(3) Å) and Cu1–N2 (1.940(3) Å) are longer than those of the Ni complexes **2a** and **2c** (Table 2), [(acac)Ni{ μ -C₆H₂(=NCH₂*t*-Bu)₄}Ni(acac)],^{39e} and [(acac)Ni{ μ -C₆H₂(=NCH₂Ph)₄}Ni(acac)],¹¹ but shorter than those of the Pd complex [(acac)Pd{ μ -C₆H₂(=NCH₂*t*-Bu)₄}Pd(acac)] (1.984(2), 1.987(3) Å).¹¹ The bond length N1–C1 (1.313(4) Å) in **3c** is shorter than that in the ligand **1c** (1.341(4) Å). The phenyl rings of the N-substituents are almost oriented essentially orthogonal to the plane formed by the four N atoms (ranging between 80.1° and 93.5°).

The UV–vis spectral data of ligands **1** and Ni and Cu complexes **2** and **3** are reported in Table 4. The UV–vis spectra of free ligands **1a**, **1b**, and **1c** show an intense absorption band at 394, 399, and 352 nm, respectively, corresponding to the

$\pi \rightarrow \pi^*$ intraquinone charge transfer.⁴³ In contrast to the free ligands **1**, the UV–vis spectra of the Ni complexes **2a–c** show two strong absorptions in the range 500–600 nm, corresponding to the $\pi \rightarrow \pi^*$ intraquinone charge transfer and a MLCT.^{11,39e} A significant red shift is observed from the δ -donor alkyl group substituted Ni complexes to π -acceptor N-substituted complexes **2**, which is attributed to an extension of the delocalization of the π -system over the Ar substituents on the N atoms.¹¹ Similar to the Ni complexes **2a–c**, the Cu complexes **3a–c** also show two strong absorptions in the range 350–500 nm, corresponding to the $\pi \rightarrow \pi^*$ intraquinone charge transfer and a MLCT, but with a significant blue shift in comparison to the Ni complexes **2a–c**.

The cyclic voltametric behavior of complexes **2c** and **3c** has been studied. The Ni complex **2c** shows two quasi-reversible redox waves at 0.03 and 0.25 V versus Fc⁺/Fc (ferrocinium/ferrocene) resulting from two successive one-electron oxidation processes (anhydrous CH₂Cl₂, N(*n*-Bu)₄PF₆ as supporting electrolyte; see Figure 5). As expected, the more electron-rich **2c** is easier to oxidize than the Ni complex [(acac)Ni{ μ -C₆H₂(=NCH₂*t*-Bu)₄}Ni(acac)] (0.03 vs 0.15 V).^{39e} Similar to **2c**, the Cu complex **3c** also shows two quasi-reversible redox waves at 0.23 and 0.80 V versus Fc⁺/Fc resulting from two successive one-electron oxidation processes.^{39e}

Norbornene Polymerization. The α -diimine Ni and Pd complexes and bis(imino)pyridine Fe and Co complexes with bulky aryl substituent ligands can produce high molecular weight polyethylene, because the bulky aryl substituents can prevent β -H transfer.^{1–3} The monocationic, square-planar complexes that were prepared by the reaction of diacetylacetonato-nickel(II) with a trityl salt, such as [CPh₃][B(C₆F₅)₄] or [CPh₃][SbCl₆], in the presence of the diimine ligands can catalyze the homopolymerization of ethylene to give branched PE products ranging from HD- to LLD-PE grades.^{2f} All the Ni and Cu complexes **2a–c** and **3a–c** bearing bulky steric hindrance π -acceptor aryl group N-substituents were synthesized, which possess two potentially reactive sites susceptible of showing cooperative effects. We think that the binuclear complexes are interesting candidates for catalytic ethylene polymerization reactions. Unfortunately, upon activation with MAO, the Ni complexes **2a–c** cannot catalyze ethylene to produce high molecular weight polyethylene at atmospheric pressure or even under 7 bar of ethylene. All the Cu complexes were completely inactive for ethylene polymerization in the presence of MAO.

To our knowledge, only a few binuclear Ni^{II} and Pd^{II} complexes with bridging ligands have been used in norbornene polymerization.^{20,44} Lee reported that bimetallic salicylaldimine-nickel catalysts show higher activities and higher polar monomer incorporations in the ethylene/2-(methoxycarbonyl)norbornene and ethylene/2-(acetoxymethyl)norbornene copolymerizations than the mononuclear complex.⁴⁵ There is no binuclear Cu complex that has been used in the addition polymerization of norbornene.

Preliminary experiments have indicated that neither binuclear Ni and Cu complexes nor MAO alone is able to catalyze norbornene polymerization. Interestingly, in combination with MAO, the Ni complexes **2a–c** exhibit extremely high catalytic activity for norbornene polymerization under moderate conditions, while the Cu complexes **3a–c** show moderate activity

(44) Hu, T.; Li, Y.; Li, Y.-X.; Hu, N.-H. *J. Mol. Catal. A: Chem.* **2006**, *253*, 155–164.

(45) S, S.; Joe, D. J.; Na, S. J.; Park, Y. W.; Choi, C. H.; Lee, B. Y. *Macromolecules* **2005**, *38*, 10027–10033.

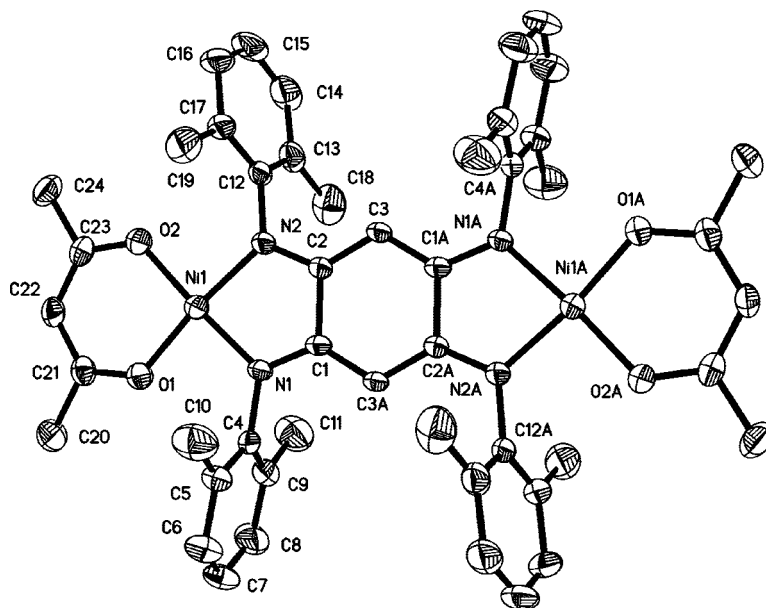


Figure 3. Molecular structure of the Ni complex **2c** with thermal ellipsoids at the 30% probability level. All H atoms have been omitted for clarity. The symmetry codes are A: $-x+1, -y+2, -z+2$.

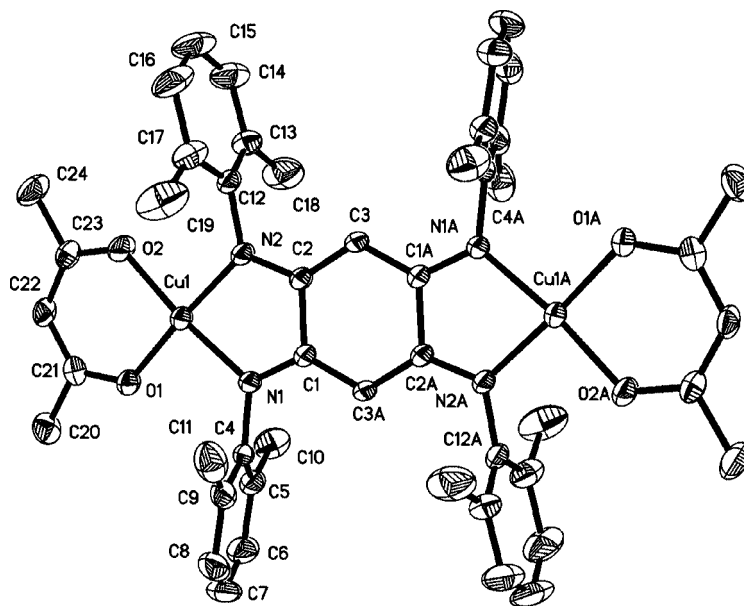


Figure 4. Molecular structure of the Cu complex **3c** with thermal ellipsoids at the 30% probability level. All H atoms have been omitted for clarity. The symmetry codes are A: $-x+1, -y+2, -z+2$.

Table 4. UV-vis Spectra Data, λ (nm), of the Ligands **1** and Complexes **2** and **3** in CH_2Cl_2

compound	λ (log ϵ)
1a	394(4.39)
1b	399(4.27)
1c	352(4.22)
2a	516(4.21), 559(4.33)
2b	509(4.08), 547(4.21)
2c	511(4.05), 546(4.18)
3a	385(4.15), 473(4.22)
3b	406(4.07), 462(4.19)
3c	405(4.04), 427(4.15)

for norbornene polymerization. The norbornene polymerization results are summarized in Tables 5 and 6.

All the binuclear Ni complexes activated with MAO display higher activities ($(4.25\text{--}6.64) \times 10^7$ g PNB mol $^{-1}$ Ni h $^{-1}$, entries 1–3 in Table 5) than the mononuclear nickel acetylacetonate

(1.28×10^7 g PNB mol $^{-1}$ Ni h $^{-1}$, entry 4 in Table 5) under similar conditions. Although the activities of the Ni complexes **2a–c** are on the same order of magnitude ($(4.25\text{--}6.64) \times 10^7$ g PNB mol $^{-1}$ Ni h $^{-1}$), the activities increase with the increase of the steric hindrance by the N-substituents (**2a** < **2b** < **2c**). However, the molecular weight of the PNB obtained by complexes **2a–c** decreases with the steric hindrance of the N-substituents ($(1.52\text{--}0.95) \times 10^6$ g mol $^{-1}$). To further investigate the norbornene polymerization behavior of these catalyst precursors, polymerizations were also investigated under varied reaction conditions. **2c** has the highest activity of the three Ni complexes (**2a–c**) and was the best choice to evaluate the effects of the MAO/Ni and the temperature on the activity and polymer molecular weights. As shown in Table 5 and Figure 6, when MAO/Ni = 250, there is almost no polymer. The catalytic activity increases from 0.58×10^7 to 6.64×10^7 g PNB mol $^{-1}$

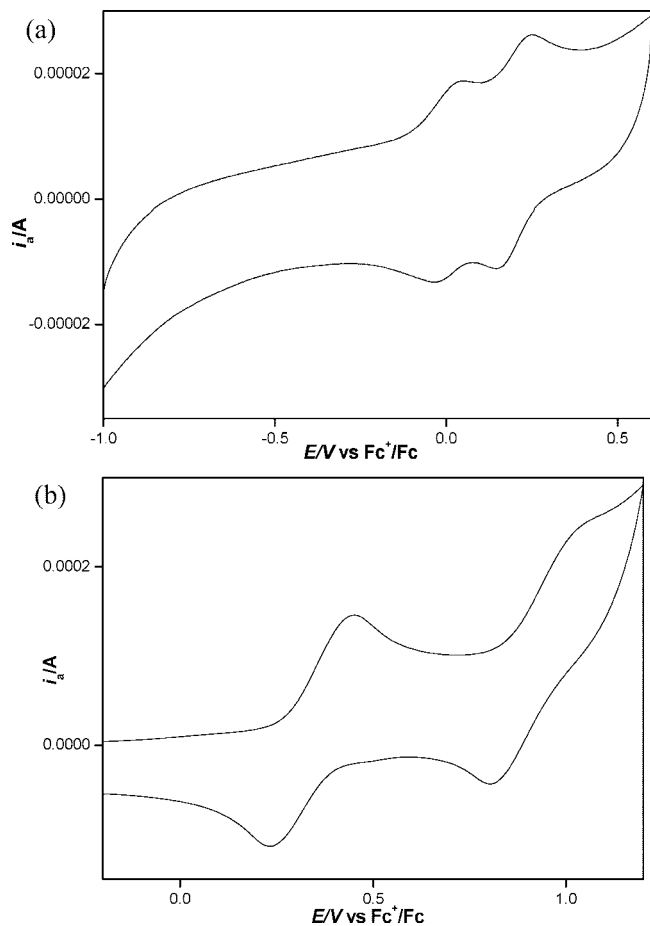


Figure 5. Cyclic voltammograms of **2c** (a) and **3c** (b) in anhydrous CH_2Cl_2 (0.1 M $\text{N}(\text{n-Bu})_4\text{PF}_6$) at a scan rate of 100 mV s^{-1} .

Table 5. Norbornene Polymerization for the 2/MAO Catalytic System^a

entry	cat.	[Ni] (μmol)	MAO/Ni	T ($^\circ\text{C}$)	yield (g)	activity ^b	M_v^c
1	2a	0.4	1250	28	1.42	4.25	1.52
2	2b	0.4	1250	28	1.54	4.60	1.41
3	2c	0.4	1250	28	2.30	6.64	0.95
4	$\text{Ni}(\text{acac})_2$	1	1250	28	2.13	1.28	1.17
5	2c	0.4	250	28	trace		
6	2c	0.4	500	28	0.31	0.58	1.94
7	2c	0.4	750	28	0.54	1.04	1.87
8	2c	0.4	1000	28	1.57	3.20	1.56
9	2c	0.4	1500	28	1.07	3.15	0.82
10	2c	0.4	2000	28	0.62	1.79	0.75
11	2c	0.4	2500	28	0.95	2.29	0.69
12	2c	0.4	1250	50	0.90	2.59	0.88
13	2c	0.4	1250	70	0.07	0.22	0.46

^a Polymerization conditions: $[\text{NB}]/[\text{Ni}] = 1 \times 10^5$; time = 5 min; $V_{\text{total}} = 20 \text{ mL}$; solvent: chlorobenzene. ^b $10^7 \text{ gPNBmol}^{-1} \text{ Ni h}^{-1}$. ^c 10^6 g mol^{-1} .

Ni h^{-1} when MAO/Ni increases from 500:1 to 1250:1. In contrast, the viscosity-average molecular weight (M_v) of the polymer decreases from 1.94×10^6 to $0.95 \times 10^6 \text{ g mol}^{-1}$ with the increase in the molar ratio of MAO to **2c** due to the chain transfer to MAO. However, when MAO/Ni increases from 1500:1 to 2500:1, the activity appears as a wavy shape, first decreasing to $1.79 \times 10^7 \text{ g PNB mol}^{-1} \text{ Ni h}^{-1}$ then increasing to $2.29 \times 10^7 \text{ g PNB mol}^{-1} \text{ Ni h}^{-1}$, while the viscosity-average molecular weight of the polymer also decreases. The temperature also influences the catalytic activity of **2c** and the molecular weights of the PNB. As shown in Table 5, with the increase in

Table 6. Norbornene Polymerization for the 3/MAO Catalytic System^a

entry	cat.	[Cu] (μmol)	MAO/[Cu]	T ($^\circ\text{C}$)	yield (g)	activity ^b	M_v^c
1	3a	7.0	500	25	0.049	0.7	6.6
2	3b	7.0	500	25	0.12	1.7	6.4
3	3c	7.0	500	25	0.45	6.5	5.9
4	$\text{Cu}(\text{acac})_2$	7.0	500	25	trace		
5	3c	7.0	50	25	trace		
6	3c	7.0	250	25	0.38	5.4	12.2
7	3c	7.0	750	25	0.24	3.4	4.8
7	3c	7.0	1000	25	0.23	3.3	2.5
8	3c	7.0	1250	25	0.27	3.9	2.3
9	3c	7.0	1500	25	0.24	3.5	2.1
10	3c	7.0	500	40	0.16	2.3	5.2
11	3c	7.0	500	60	0.03	0.5	1.2
12	3c	7.0	500	80	trace		

^a Polymerization conditions: $[\text{NB}]/[\text{Cu}] = 1 \times 10^4$; time = 1 h; $V_{\text{total}} = 20 \text{ mL}$; solvent: chlorobenzene. ^b $10^4 \text{ g PNB mol}^{-1} \text{ Cu h}^{-1}$. ^c 10^5 g mol^{-1} .

the reaction temperature, both the catalytic activity and the molecular weight decrease significantly. At $28 \text{ }^\circ\text{C}$ the highest activity, up to $6.64 \times 10^7 \text{ g PNB mol}^{-1} \text{ Ni h}^{-1}$, and M_v , up to $0.95 \times 10^6 \text{ g mol}^{-1}$, are obtained. These Ni binuclear complexes **2a–c** are as highly active as recently described nickel^{41,6,37a,44} complexes and $\text{Pd}^{23,18,24}$ complexes and show a higher polymerization activity than the mononuclear bis(imino)pyridyl nickel^{21e} complex and other early transition metal and copper complexes.^{12–21,37a}

For Cu complexes **3a–c**, the catalytic activity is lower than for the corresponding Ni complexes **2a–c** (Figure 6). As shown in Table 6, among the Cu complexes **3a–c**, complex **3c** has the highest activity ($6.5 \times 10^4 \text{ g PNB mol}^{-1} \text{ Cu h}^{-1}$). The mononuclear copper acetylacetonate showed no activity under the same conditions.³⁴ The MAO/Cu ratios also affect the activity and molecular weights (Figure 6). When MAO/Cu = 500, the activity of **3c** achieved the maximum value ($6.5 \times 10^4 \text{ g PNB mol}^{-1} \text{ Cu h}^{-1}$). As the MAO/Cu ratios increase, the activity of **3c** achieved $3.4 \times 10^4 \text{ g PNB mol}^{-1} \text{ Cu h}^{-1}$ (MAO/Cu = 750), while the M_v of the polymer decreased sharply from $4.8 \times 10^6 \text{ g mol}^{-1}$ to $2.1 \times 10^6 \text{ g mol}^{-1}$. Similar to the Ni complex **3c**, the reaction temperature also influences the activity and the molecular weights of the PNB. At $25 \text{ }^\circ\text{C}$, the highest activity, up to $6.5 \times 10^4 \text{ g PNB mol}^{-1} \text{ Cu h}^{-1}$, and M_v , up to $5.9 \times 10^6 \text{ g mol}^{-1}$, are obtained, while at $70 \text{ }^\circ\text{C}$, there is no polymer obtained, which is different from bis(salicylaldimine)copper(II) complexes.³⁴

The microstructure of the obtained PNB by the binuclear Ni complexes **2a–c** and Cu complexes **3a–c** is characterized by FTIR spectra and ^1H NMR and ^{13}C NMR spectra. The spectra are similar and are typical of an addition-type structure. In the FTIR spectra (IR (KBr): 2946, 2868, 1474, 1451, 1372, 1296, 1258, 1221, 1190, 1148, 1108, 1041, 942, 893, 806, 730 cm^{-1}), there are no absorptions at $1680\text{--}1620 \text{ cm}^{-1}$, especially around 960 and 735 cm^{-1} , assigned to the *trans* and *cis* form of double bonds, respectively, which are characteristic of the ROMP structure of PNB.¹⁹

^1H NMR and ^{13}C NMR spectra (Supporting Information) confirmed the above conclusions. ^1H NMR spectra (^1H NMR: δ 0.9–3.0 (m, maxima at 1.14, 1.21, 1.56, 2.30, 2.37 ppm)) show signals in the 0.9–3.0 ppm range, where no resonances are displayed at about 5.1 and 5.3 ppm in the ^1H NMR spectrum of the PNB, assigned to the *cis* and *trans* form of the double bonds,¹⁹ which generally indicates the presence of the ring-opening metathesis polymerization (ROMP) structure. The ^{13}C NMR spectrum shows the main four broad groups of resonances,

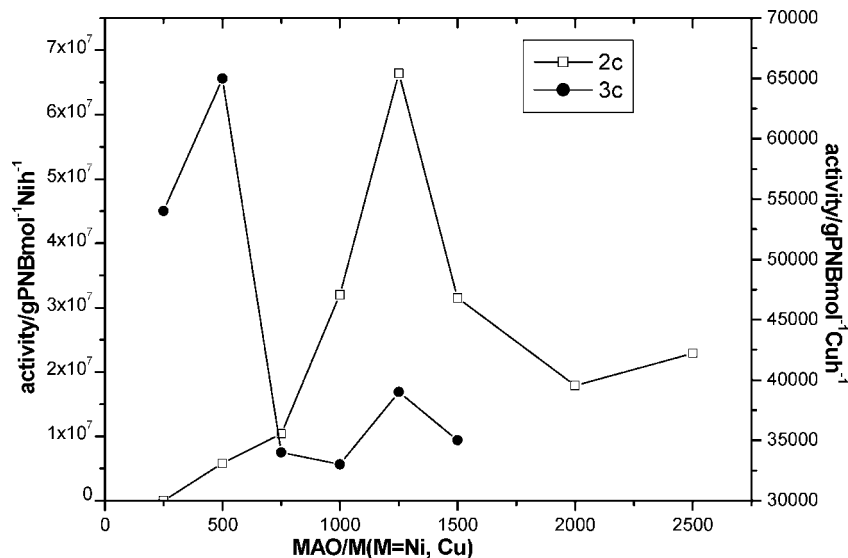
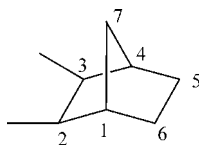


Figure 6. Influence of MAO/M (M = Ni, Cu) on the activity of polymerization of NB with **2c** and **3c**. Detailed conditions are given in Tables 5 and 6.

Scheme 2



δ (49–46.3), (37–38), (34), (30) ppm, attributed to carbons 2 and 3, carbons 1 and 4, carbon 7, and carbons 5 and 6, respectively (Scheme 2).¹⁹ These data indicate that the polynorbornene obtained with the aforementioned catalysts was an addition-type (2,3-linked) product. Their ¹³C NMR spectra show that both polymers are *exo* enchainment; the spectra do not exhibit resonances in the 20–24 ppm region.¹⁹ We attribute the tacticity in these spectra to differences in polymer architectures. Unfortunately, the broad, unresolved nature of the spectra (PNB is more stiff with hindered rotation than the ethene-norbornene copolymer) made it difficult to assign exact stereochemistry to the enchainment of norbornene in the polymers with absolute certainty.^{21a} Our attempts to determine the glass transition temperature (T_g) of PNB failed, and the DSC studies did not give an endothermic signal upon heating to the decomposition temperature (above 450 °C).

MMA Polymerization. To our best knowledge, there is only one binuclear nickel complex used in MMA polymerization.^{27a} Neither when **2a–c** and **3a–c** were used in the absence of MAO nor when MAO alone was employed was any catalytic activity at room temperature ascertained in the polymerization of MMA; therefore, all the other experiments were carried out in the presence of both components. All the Ni complexes **2a–c** activated with MAO exhibit high activity for MMA polymerization. In contrast, the Cu complexes **3a–c** in combination with MAO resulted in almost no polymer at room temperature even after 24 h.

Table 7 shows the results of MMA polymerization with different binuclear Ni complexes **2a–c** and Ni(acac)₂ under the same conditions. After activation with MAO, all the Ni complexes can catalyze polymerization of MMA to produce high syndiotactic-rich PMMA (all the *rr* values exceed 70%, the highest up to 74.6% for complex **2b**, entry 2, Table 7) with high activities (4.5 × 10⁴ g PMMA mol⁻¹ Ni h⁻¹ for complex **2c**). All the binuclear nickel complexes **2a–c** produced PMMA

Table 7. MMA Polymerization with Different Nickel Complexes^a

entry	catalyst	yield (g)	activity ^b	% <i>mm</i>	% <i>mr</i>	% <i>rr</i>	$M_n^{c,d}$	$M_w^{c,d}$	M_w/M_n^c
1	2a	0.78	3.9	6.3	23.2	70.4	1.15	5.79	5.0
2	2b	0.84	4.2	6.7	18.6	74.6	0.75	5.15	6.8
3	2c	0.90	4.5	5.8	21.1	73.1	1.39	4.98	3.6
4	Ni(acac) ₂	0.56	2.8	11.9	37.6	50.6	0.74	6.06	8.2

^a Polymerization conditions: Ni = 20 μmol, MAO/Ni = 50, MMA = 28.5 mmol, toluene = 12 mL, $T = 27$ °C, time = 1 h. ^b 10⁴ g PMMA mol⁻¹ Ni h⁻¹. ^c Determined by GPC analysis. ^d 10⁵ gmol⁻¹.

with similar microstructures, and the analyses of the *rr*, *mr*, and *mm* stereotriad distributions indicated that these catalytic systems initiate MMA polymerization to yield PMMA with syndiotactic-rich atactic microstructures (*rr* content is between 70.4 and 74.6%). The variation of N-substituents on the ligand group has little influence on the syndiotacticity of PMMA. The values of the syndiotacticity degree (*rr* triads >70%) are comparable to or higher than the PMMA obtained by the Ni(acac)₂ complexes (*rr* triads 50.6%) and Ni complexes bearing N,O-chelate ligands²⁷ and other nickel complexes^{28,29} or (pyridyl bisimine)iron(II) and -cobalt(II) complexes.^{29d} Although there is a different steric hindrance of complexes **2a**, **2b**, and **2c**, the catalytic activities of the three complexes are of the same magnitude. It is indicated that the N-substituents on the bridging fragment have little influence on the catalytic activity toward MMA polymerization. The binuclear Ni complexes **2a–c** exhibit higher activities than the corresponding mononuclear complex Ni(acac)₂ (2.8 × 10⁴ g PMMA mol⁻¹ Ni h⁻¹)^{29a,c} and the Ni(II) α -diimine/MAO and Fe(II) and Co(II) pyridyl bis(imine)/MAO systems.^{29d} The PMMA catalyzed by **2a–c** showed high number-average molecular weight ($M_n = (0.75\text{--}1.39) \times 10^5$ g mol⁻¹) and broad molecular weight distribution (PDI) ($M_w/M_n = 3.6\text{--}6.8$). The observed effects on broad molecular weight distribution can also be explained on the basis of electronic effects and cooperative interactions of the two adjacent nickel centers in conjugate binuclear complex systems. These two metal centers are electronically coupled through the ligand bridge. The interaction between two metals made it possible to create more than one kind of active species during the polymerization.^{4h} However, the PMMA obtained by the Ni(acac)₂/MAO system exhibits a wide molecular weight distribution (8.2, Table 7), which is consistent with the literature.^{29c}

Table 8. Influence of MAO/Ni on the Polymerization of MMA with **2c**/MAO^a

entry	MAO/Ni	yield (g)	activity ^b	% <i>mm</i>	% <i>mr</i>	% <i>rr</i>	$M_n^{c,d}$	$M_w^{c,d}$	M_w/M_n^c
1	12.5	0.47	2.35	6.1	17.5	76.4	0.52	4.48	8.6
2	25	0.62	3.10	7.2	18.6	74.1	0.65	4.20	6.5
3	50	0.90	4.50	5.8	21.1	73.1	1.39	4.98	3.6
4	100	0.98	4.90	7.6	23.4	68.9	1.55	4.92	3.18
5	150	1.05	5.25	10.1	30.7	59.2	0.95	3.55	3.73

^a Polymerization conditions: Ni = 20 μ mol, MMA = 28.5 mmol, toluene = 12 mL, $T = 27$ °C, time = 1 h. ^b 10^3 g PMMA mol⁻¹ Ni h⁻¹. ^c Determined by GPC analysis. ^d 10^5 g mol⁻¹.

Table 9. Influence of the Temperature on the Polymerization of MMA with **2c**/MAO^a

entry	T (°C)	yield (g)	activity ^b	% <i>mm</i>	% <i>mr</i>	% <i>rr</i>	$M_n^{c,d}$	$M_w^{c,d}$	M_w/M_n^c
1	4	0.06	0.30	7.3	19.1	73.5	n.d.	n.d.	n.d.
2	27	0.90	4.50	5.8	21.1	73.1	1.39	4.98	3.6
3	50	0.67	3.35	6.6	19.8	73.5	0.60	4.45	7.4
4	75	0.44	2.20	8.6	25.2	56.3	0.77	4.62	6.0

^a Polymerization conditions: Ni = 20 μ mol, MMA = 28.5 mmol, toluene = 12 mL, MAO/Ni = 50; time = 1 h. ^b 10^4 g PMMA mol⁻¹ Ni h⁻¹. ^c Determined by GPC analysis. ^d 10^5 g mol⁻¹.

Taking into account that the viscosity of the medium gradually increased during polymerization, diffusion phenomena could be responsible for the wide molecular weight distribution.^{27c,f}

In the polymerizations of ethylene and norbornene with metallocene- and later transition metal-MAO catalysts, a large MAO/metal ratio is necessary to give high catalytic activity,¹ while the Ni(acac)₂-MAO and other catalysts on polymerization of MMA have the advantage of requiring a smaller amount of MAO (MAO/Ni = 10–200) to reach high activity.²⁹ To check this point, the effect of the MAO/Ni ratio on the polymerization of MMA with the binuclear nickel complex **2c** catalyst was examined. As shown in Table 8, it is clear that a large amount of MAO is not required to reach high polymerization activity. The polymerization rate increased with an increase of MAO/Ni up to 50 and then remained almost constant. The MAO/Ni ratio influences the stereotacticity, molecular weight, and molecular weight distribution. With the increase of MAO/Ni, the PMMA stereotriad distribution with *rr* value and PDI value decreases (Table 8), while the molecular weight increases.

The temperature also affects considerably the catalytic activities, microstructure, and molecular weight as well as molecular weight distribution (Table 9). The catalytic activity of **2c** first increased and then decreased with increasing polymerization temperature, and the highest activity values were achieved at room temperature. The *rr* values are keep almost constant when the temperature is between 4 and 50 °C, but sharply drop to 56.3% when the temperature is 75 °C. The number-average molecular weight decreases with increasing temperature; however, the PDI increased.

The obtained syndiotactic-rich atactic PMMA catalyzed by the binuclear Ni complexes **2a–c** was different from the atactic PMMA (low *rr* value) produced by the lanthanide complexes.⁴⁶ Recently, there are an increasing number of papers suggesting that transition metal catalyzed polymerization of acrylates is not a coordination–insertion mechanism, but rather follows a

free radical polymerization mechanism.⁴⁷ According to the results that the distributions of *rr*, *mr*, and *mm* stereotriads of the atactic microstructure are similar to those of PMMA prepared with a free radical initiator⁴⁸ and detected by the radical traps, the radical polymerization mechanism for methyl acrylate polymerization catalyzed by the neutral palladium complex bearing pyrrole-imine ligands^{47a} and neutral palladium complexes [Pd(C₆F₅)Br(NCMe)₂]^{47b} and [Pd₂(μ -X)₂(C₆F₅)₂L₂] [L = tetrahydrothiophene (tht), X = Cl]^{47c} has been reported. Wu^{49a} suggested that the polymerization of MMA with bis(β -ketoamino)nickel(II)-MAO catalyst runs using a radical polymerization mechanism. However, Li^{49b} reported that the polymerization of MMA (syndiotactic-rich atactic PMMA) catalyzed by the neutral nickel complexes bearing β -ketoamino chelate ligands did not occur via a radical mechanism, as the adding galvinoxyl as a free radical inhibitor cannot halt the polymerization. Carlini^{27b,d,f} also obtained similar results by using salicylaldiminate nickel complexes and MAO. However, Sen⁵⁰ pointed out that the use of radical traps such as galvinoxyl, DPPH, and TEMPO as probes for a radical mechanism in metal-base systems such as Cu(DMOX)Cl₂ and Ni(acac)₂ employing MAO can lead to the wrong conclusion. The radical traps may fail to intercept even radical reactions that proceed in the presence of MAO. Endo^{29a} suggested that the polymerization of MMA by the Ni(acac)₂/MAO system proceeds by a coordination–insertion mechanism. The high values of *rr* triad syndiotacticity degree of the PMMA obtained by the binuclear nickel complexes **2a–c** and MAO, which can catalyze oligomerization of ethylene,¹¹ seem to suggest that the polymerization process could proceed mainly with a metal coordinative mechanism, although a free radical mechanism cannot be completely excluded.

Conclusion

Binuclear, divalent nickel and copper acetylacetonato complexes **2** and **3** with bulky sterically hindered N-substituent $6\pi + 6\pi$ amine-imine ligands have been synthesized. The crystal structures of the complexes **2a**, **2c**, and **3c** were similar in that in all the complexes the geometry of the metal ions is square-planar, and a complete electronic delocalization of the quinonoid π -system occurs between the metal centers over the two N=C–C=C=N halves of the ligand. The cyclic voltametric behavior of the complexes **2c** and **3c** has been studied. The binuclear nickel complexes **2a–c** activated with MAO exhibit highly catalytic activity for norbornene addition–polymerization (the maximum activity is 6.64×10^7 g PNB mol⁻¹ Ni h⁻¹) and MMA polymerization (the highest activity is 4.5×10^4 g PMMA mol⁻¹ Ni h⁻¹), while the copper complexes exhibit moderate activity for norbornene addition–polymerization and are inactive for MMA polymerization. The PMMA obtained by the binuclear nickel complexes are syndiotactic-rich and have broad PDI.

(47) (a) Tian, G.; Boone, H. W.; Novak, B. M. *Macromolecules* **2001**, *34*, 7656–7663. (b) Elia, C.; Sharon, E. B.; Sen, A. *Organometallics* **2002**, *21*, 4249–4256. (c) Albéniz, A. C.; Espinet, P.; Raquel, L. F. *Organometallics* **2003**, *22*, 4206–4212.

(48) Frisch, H. L.; Mallovs, C. L.; Heatley, F.; Bovey, F. A. *Macromolecules* **1968**, *1*, 533.

(49) (a) He, X.-H.; Wu, Q. *Appl. Organomet. Chem.* **2006**, *20*, 264. (b) Li, X.-F.; Li, Y.-G.; Li, Y.-S.; Chen, Y.-X.; Hu, N.-H. *Organometallics* **2005**, *24*, 2502–2510.

(50) Nagel, M.; Paxton, W. F.; Sen, A.; Zakharov, L.; Rheingold, A. *Macromolecules* **2004**, *37*, 9305–9307.

(46) (a) Woodman, T. J.; Schormann, M.; Hughes, D. L.; Bochmann, M. *Organometallics* **2004**, *23*, 2972–2979. (b) Woodman, T. J.; Schormann, M.; Bochmann, M. *Organometallics* **2003**, *22*, 2938–2943. (c) Woodman, T. J.; Schormann, M.; Hughes, D. L.; Bochmann, M. *Organometallics* **2003**, *22*, 3028–3030.

Experimental Section

General Procedures. All air-sensitive experiments were carried out under nitrogen using standard Schlenk techniques. Solvents were dried prior to use by refluxing over and distillation from sodium (THF, toluene, hydrocarbons) or calcium hydride (dichloromethane, chlorobenzene). Norbornene (Acros) was purified by distillation over sodium and used as a solution in chlorobenzene. MMA was purified by drying from CaH₂ and distilled under vacuum. Methylaluminoxane (MAO) was purchased from Aldrich as 10% weight of a toluene solution and used without further purification. 1,2,4,5-Tetrabromobenzene and 2,6-dimethylaniline (98%) were purchased from Aldrich. Other chemicals were of analytical grade and were used as received. FTIR spectra were recorded on a Nicolet FT-IR spectrometer. Elemental analyses were performed on an Elementar Vario EL III analyzer. ¹H and ¹³C NMR spectra were carried out on a Bruker AC 500 spectrometer at room temperature in CDCl₃ solution for ligands and polymers using TMS as internal standard. UV/vis spectra were recorded at room temperature with a Kontron Instruments UVIKON 860. Electrochemical experiments were performed with a three-electrode system consisting of a platinum working electrode, a platinum wire counter electrode, and a silver wire as pseudoreference electrode. All potentials are reported versus the Fc⁺/Fc couple. The measurements were carried out under Ar, in degassed CH₂Cl₂ (distilled from CaH₂ under N₂), using 0.1 M N(*n*-Bu)₄PF₆ as the supporting electrolyte. Gel permeation chromatography (GPC) analyses of the molecular weight and molecular weight distribution of the PMMA were performed on an Agilent 1100 instrument using standard polystyrene as calibration and with THF as the eluent at 35 °C. The tacticity of PMMA was determined by the α -methyl resonance of the ¹H NMR.⁵¹

Synthesis of Ligand *N,N,N',N'*-Tetra(*p*-methylphenyl)-*p*-benzoquinonediimine (1a).⁴⁰ A 100 mL Schlenk flask was charged with 1,3-bis(2,6-diisopropylphenyl)imidazolium chloride (0.1 mmol), NaOt-Bu (0.1 mmol), Pd(OAc)₂ (0.05 mmol), and PhCH₃ (60 mL). After stirring the resulting mixture for 20 min at 80 °C, 1,2,4,5-tetrabromobenzene (5.00 mmol), *p*-PhCH₃NH₂ (35 mmol), and NaOt-Bu (20 mmol) were added. The resulting mixture was sealed under an atmosphere of nitrogen and stirred at 110 °C for 14 h. After cooling to room temperature, the resulting mixture was diluted with hexanes and precipitated solids were collected by filtration. Residual inorganic salts were removed by filtering CH₂Cl₂ solutions of the mixture and stirred at room temperature under oxygen atmosphere for 2 days followed by removal of the solvent to obtain a brick red product (1.49 g, 60%). ¹H NMR (CDCl₃): δ 8.19 (s, 2H), 7.11–7.33 (br, 8H), 6.93–6.99 (br, 8H), 6.25 (s, 2H), 2.32 (s, 12H). IR (KBr): ν (N–H) 3317 cm⁻¹. Anal. Calcd for C₃₄H₃₂N₄: C 82.22, H 6.49, N 11.28. Found: C 82.12, H 6.29, N 11.21. UV–visible (CH₂Cl₂) λ (log ϵ): 394 nm (4.39).

Synthesis of Ligand *N,N,N',N'*-Tetra(*o*-methylphenyl)-*p*-benzoquinonediimine (1b). The synthesis procedure was similar to that for the ligand **1a** to afford the brick red solid **1b** (62%). ¹H NMR (CDCl₃): δ 8.23 (s, 2H), 7.14–7.19 (br, 8H), 6.98 (br, 8H), 5.95 (s, 2H), 2.22 (s, 12H). IR (KBr): ν (N–H) 3240 cm⁻¹. Anal. Calcd for C₃₄H₃₂N₄: C 82.22, H 6.49, N 11.28. Found: C 81.79, H 5.96, N 10.97. UV–visible (CH₂Cl₂) λ (log ϵ): 399 nm (4.27).

Synthesis of Ligand *N,N,N',N'*-Tetra(2,6-dimethylphenyl)-*p*-benzoquinonediimine (1c). The synthesis procedure was similar to that for the ligand **1a** to afford the orange solid **1c** (59%). ¹H NMR (CDCl₃): δ 7.84 (s, 2H), 6.95 (br, 12H), 4.56 (s, 2H), 2.09 (s, 24H). IR (KBr) ν (N–H) 3291 cm⁻¹. Anal. Calcd for C₃₈H₄₀N₄: C 82.61, H 7.21, N 10.14. Found: C 82.54, H 7.06, N 9.91. UV–visible (CH₂Cl₂) λ (log ϵ): 352 nm (4.22).

Synthesis of Ni Complex [Ni(acac){ μ -C₆H₂(=N(*p*-CH₃-Ph))₄}Ni(acac)] (2a). Ligand **1a** (0.344 mmol) was dissolved in CH₂Cl₂ (80 mL), and Ni(acac)₂ (0.688 mmol) was added; the brown-red solution turned immediately to intense purple. The reaction mixture was stirred at room temperature for 24 h. The solution was concentrated to about 40 mL, 20 mL of *n*-hexane was added, and the solution was then filtered and washed with *n*-hexane (3 \times 15 mL), to afford an intense purple solid. Yield: 0.21 g, 78%. The crystal of **2a** was obtained by slow evaporation from CH₂Cl₂/hexane (10:1) solution. ¹H NMR (CDCl₃): δ 6.81–6.87 (br, 16H, CH-aryl), 5.11 (s, 2H, CH-acac), 4.38 (s, 2H, N=C=C–H), 2.14 (s, 12H, PhCH₃), 1.33 (s, 12H, CH₃-acac). IR (KBr): ν (cm⁻¹) 3082, 3019, 2970, 2920, 2864, 1582, 1519, 1387, 1309, 1285, 1205, 1170, 1102, 1072, 1022, 933, 881, 814, 794, 769, 707. Anal. Calcd for C₄₄H₄₄N₄O₄Ni₂: C 65.22, H 5.47, N 6.91. Found: C 65.03, H 5.32, N 7.08. UV–visible (CH₂Cl₂) λ (log ϵ): 516 nm (4.21), 559 nm (4.33).

Synthesis of Ni Complex [Ni(acac){ μ -C₆H₂(=N(*o*-CH₃-Ph))₄}Ni(acac)] (2b). The procedure was similar to the synthesis of **2a** using ligand **1b** and Ni(acac)₂, affording complex **2b** as an intense purple solid. Yield: 74.3%. ¹H NMR (CDCl₃): δ 6.89 (br, 16H, CH-aryl), 5.07 (s, 2H, CH-acac), 3.78 (s, 2H, N=C=C–H), 2.39 (s, 12H, CH₃-aryl), 1.23 (s, 12H, CH₃-acac). IR (KBr): ν (cm⁻¹) 3067, 3017, 2916, 1579, 1512, 1426, 1388, 1309, 1280, 1185, 1111, 1024, 882, 798, 772, 716, 747. Anal. Calcd for C₄₄H₄₄N₄O₄Ni₂: C 65.22, H 5.47, N 6.91. Found: C 65.01, H 5.38, N 6.75. UV–visible (CH₂Cl₂) λ (log ϵ): 509 nm (4.08), 547 nm (4.21).

Synthesis of Ni Complex [Ni(acac){ μ -C₆H₂(=N(2,6-(CH₃)₂-Ph))₄}Ni(acac)] (2c). The procedure was similar to the synthesis of **2a** using ligand **1c** and Ni(acac)₂ and afforded complex **2c** as an intense purple solid. Yield: 82%. ¹H NMR (CDCl₃): δ 6.76–6.78 (br, 12H, CH-aryl), 5.04 (s, 2H, CH-acac), 3.57 (s, 2H, N=C=C–H), 2.40 (s, 24H, CH₃-aryl), 1.18 (s, 12H, CH₃-acac). IR (KBr): ν (cm⁻¹) 3067, 3021, 2970, 2914, 1577, 1511, 1473, 1385, 1303, 1290, 1178, 1086, 1029, 973, 871, 794, 753. Anal. Calcd for C₄₈H₅₂N₄O₄Ni₂: C 66.50, H 6.00, N 6.46. Found: C 66.25, H 5.69, N 6.36. UV–visible (CH₂Cl₂) λ (log ϵ): 511 nm (4.05), 546 nm (4.18).

Synthesis of Cu Complex [Cu(acac){ μ -C₆H₂(=N(*p*-CH₃-Ph))₄}Cu(acac)] (3a). The procedure was similar to the synthesis of **2a** using ligand **1a** and Cu(acac)₂, affording complex **3a** as an olivine solid. Yield: 64%. IR (KBr): ν (cm⁻¹) 3056, 3018, 2916, 2861, 1582, 1471, 1414, 1383, 1312, 1296, 1203, 1170, 1106, 1019, 966, 872, 811, 775, 706. Anal. Calcd for C₄₄H₄₄N₄O₄Cu₂: C 64.45, H 5.41, N 6.83. Found: C 64.28, H 5.24, N 7.04. UV–visible (CH₂Cl₂) λ (log ϵ): 385 nm (4.15), 473 nm (4.22).

Synthesis of Cu Complex [Cu(acac){ μ -C₆H₂(=N(*o*-CH₃-Ph))₄}Cu(acac)] (3b). The procedure was similar to the synthesis of **2a** using ligand **1b** and Cu(acac)₂, affording complex **3b** as an olivine solid. Yield: 59%. IR (KBr): ν (cm⁻¹) 3062, 3016, 2960, 2917, 1557, 1585, 1475, 1384, 1303, 1268, 1215, 1184, 1109, 1039, 967, 875, 811, 777, 747, 717, 627. Anal. Calcd for C₄₄H₄₄N₄O₄Cu₂: C 64.45, H 5.41, N 6.83. Found: C 64.32, H 5.24, N 6.95. UV–visible (CH₂Cl₂) λ (log ϵ): 406 nm (4.07), 462 nm (4.19).

Synthesis of Cu Complex [Cu(acac){ μ -C₆H₂(=N(2,6-(CH₃)₂-Ph))₄}Cu(acac)] (3c). The procedure was similar to the synthesis of **2a** using ligand **1c** and Cu(acac)₂, affording complex **3c** as a dark green solid. Yield: 61%. IR (KBr): ν (cm⁻¹) 3058, 3019, 2965, 2916, 2847, 2719, 1588, 1513, 1464, 1383, 1303, 1278, 1187, 1089, 1022, 937, 870, 760, 702. Anal. Calcd for C₄₈H₅₂N₄O₄Cu₂: C 65.68, H 5.98, N 6.39. Found: C 65.54, H 6.10, N 6.26. UV–visible (CH₂Cl₂) λ (log ϵ): 405 nm (4.04), 427 nm (4.15).

Ethylene Polymerization. The ethylene polymerization procedure was similar to the literature.^{4h}

Norbornene Polymerization. In a typical procedure for norbornene polymerization, precatalyst nickel or copper complex in

(51) Konishi, T.; Tamai, Y.; Fujii, M.; Einaga, Y.; Yamakawa, H. *Polym. J.* **1989**, *21*, 329.

chlorobenzene was added into a special polymerization bottle (50 mL) with a stirrer under nitrogen atmosphere. Then MAO was charged into the polymerization system via syringe. Then the norbornene in chlorobenzene was added to the polymerization system and the reaction was started. After a designated time, acidic ethanol ($V_{\text{ethanol}}:V_{\text{concd.HCl}} = 10:1$) was added to terminate the reaction. The PNB was isolated by filtration, washed with ethanol, and dried at 80 °C for 48 h under vacuum. For all polymerization procedures, the total reaction volume was 20.0 mL, which can be achieved by variation of the amount of chlorobenzene when necessary. The molecular weights of PNB were measured according to the literature.⁵²

MMA Polymerization. In a typical procedure (Table 7, entry 3), 20.0 μmol of binuclear nickel(II) complex **2a–c** in 5.0 mL of toluene and 28.5 mmol (3.0 mL) of MMA were added into a polymerization bottle with strong stirring under a nitrogen atmosphere. After the mixture was kept at 27 °C for 5 min, MAO was charged into the polymerization system by means of a syringe, and the reaction was initiated. After 1 h, acidic methanol ($V_{\text{ethanol}}:V_{\text{concd.HCl}} = 10:1$) was added to terminate the reaction. The polymer was isolated by filtration, washed with methanol, and dried at 80 °C for 48 h under vacuum.

(52) Haselwander, T.; F, A.; Heitz, W.; Maskos, M. *Macromol. Rapid Commun.* **1997**, *18*, 689–697.

X-ray Crystallography. Diffraction data of ligand **1c** and complexes **2a**, **2c**, and **3c** were collected on a Bruker Smart APEX CCD diffractometer with graphite-monochromated Mo K α radiation ($\lambda = 0.71073 \text{ \AA}$). All data were collected at room temperature, and the structures were solved by direct methods and subsequently refined on F^2 by using full-matrix least-squares techniques (SHELXL).⁵³ Absorption corrections were applied to the data. The non-hydrogen atoms were refined anisotropically, and hydrogen atoms were located at calculated positions.

Acknowledgment. Financial support by the National Science Foundation of China (20531020, 20421303, 20771028, 20601004), by the National Basic Research Program of China (2005CB623800), by Shanghai Leading Academic Discipline project (B108), and by Shanghai Science and Technology Committee (05DZ22313, 06XD14002) is gratefully acknowledged.

Supporting Information Available: Crystallographic data for **1c**, **2a**, **2c**, and **3c** are available free of charge via the Internet at <http://pubs.acs.org>.

OM700901X

(53) Sheldrick, G. M. *SHELXL-97*; Universität Göttingen: Germany, 1997.